Biomechanical Relevance of the Microstructure in Artery Walls with a Focus on Passive and Active Components

BY GERHARD A. HOLZAPFEL[1,2,*] AND RAY W. OGDEN[3]

[1]*Institute of Biomechanics, Graz University of Technology, Austria*

[2] *Norwegian University of Science and Technology (NTNU)*
Faculty of Engineering Science and Technology, Trondheim, Norway

[3]*School of Mathematics and Statistics, University of Glasgow, Scotland, UK*

Review Article Submitted to a Special Call on
'Extracellular Matrix in Cardiovascular Pathophysiology'

To appear in
The American Journal of Physiology – Heart and Circulatory Physiology

Abstract. The microstructure of arteries, consisting, in particular, of collagen, elastin and vascular smooth muscle cells, plays a very significant role in their biomechanical response during a cardiac cycle. In this paper we highlight the microstructure and the contributions of each of its components to the overall mechanical behavior. We also describe the changes of the microstructure which occur as a result of abdominal aortic aneurysms and disease such as atherosclerosis. We also focus on how the passive and active constituents are incorporated into a mathematical model without going into detail of the mathematical formulation. We conclude by mentioning open problems towards a better characterization of the biomechanical aspects of arteries that will be beneficial for a better understanding of cardiovascular pathophysiology.

Keywords: artery wall biomechanics; artery wall microstructure; artery tissue modeling; artery layers; passive–active modeling

*Author for correspondence (holzapfel@tugraz.at).

Introduction

Pathophysiological changes in the cardiovascular system directly influence the microstructure and the biomechanical response of vascular walls [56]. Diseases such as hypertension, diabetes, atherosclerosis, aneurysms or aortic dissection cause significant changes in the mechanical properties of the microstructure. It is therefore crucial to understand the mechanical properties of the individual components and their influence on the overall mechanical properties. The passive mechanical behavior of vascular walls is mainly governed by the extrafibrillar matrix (proteoglycans, water, etc.), collagen and elastic fibers, while the active mechanical contribution is due to the smooth muscle cells (SMCs), which can function to maintain vascular tone and resistance. This has stimulated the development of mechanical models that describe the tissue properties in health and disease. The matrix can be considered as an isotropic material [83, 84], while the collagen fibers generate the anisotropy of the tissue [38]. It has been shown experimentally that the collagen fibers are not perfectly aligned but are arranged in a dispersed structure for which a mean direction can be defined. The microstructure depends on the location within a vessel, and the particular vessel under consideration as well as its (patho)physiological condition. Fiber dispersion in artery walls has been identified using different imaging modalities such as second-harmonic generation and diffusion tensor imaging; see, e.g., the studies [3, 7, 16, 17, 19, 22, 28, 56, 66, 67]. In each of the main layers of an artery wall, namely the intima, media and adventitia, there are typically two families of fibers, approximately symmetrically arranged [68]. The arrangement of the two families in elastic arteries is essentially helical but in more muscular arteries, e.g., the families are arranged close to the circumferential and axial directions [14]. These arrangements and the associated mechanical properties can be severely disrupted by various diseases. SMCs also have a distinguished alignment and function which can be altered by disease, and differs in different types of arteries and species [59, 18, 57]. They generate force by contraction and this contributes significantly to the material behavior of the artery wall. Hence, in order to better understand the functioning of artery walls it is necessary to also consider muscle activation in a constitutive model.

Microstructure and Biomechanics of Artery Walls

Microstructure. Artery walls consist of three distinguished layers, i.e. the intima, media

and adventitia, which have specific content and arrangements of constituents, different functions, microstructures and biomechanical responses [59, 12, 38, 57, 56]. While the media is the main load bearing layer under physiological loading, it is the adventitia (outermost artery layer) which bears load mainly under higher blood pressure and protects the wall from overstretching [70]. The intima is also a load bearing layer but mainly in arteries with non-atherosclerotic intimal thickening because its thickness tends to increase with age; e.g., it occupies 20% or more of the infrarenal aortic wall [37, 68]. The three artery layers are mainly composed of elastin and collagen and form a composite material. In the lower pressure domain the elastin is load bearing while under higher loads the collagen is recruited and the main load is transfered to the collagen reinforcement [60]. The collagen in the layered media of elastic arteries is organized within concentric elastic lamellae. There are also three primary types of cells present in artery walls, specifically fibroblasts, mainly in the collagen-rich adventitia, abundant SMCs in the medial layer and endothelial cells, which line the luminal surface of the intima. It is the SMCs which are responsible for the activation of the blood vessel and are important for its mechanical response. These cell types are particularly sensitive to their mechanical environment; e.g., endothelial cells respond to cyclic stretching and to changes in the wall shear stress, while SMCs and fibroblasts are also sensitive to cyclic stretching. For a more detailed discussion of cellular responses see, e.g., [39].

In artery walls elastin (the main component of elastic fibers which also includes fibrillin-1 that forms a scaffold for elastin deposition) is present as thin strands. It is made up of long flexible molecules that form a 3D network, and may be stretched to more than double its initial length. Elastin behaves like a rubber-like material and can sustain very large strains under low stresses without rupturing, but then fractures while still under relatively low stresses. While elastin has generally been assumed to be isotropic it has been suggested that the assumption of isotropy is not always justified [88, 84]. In artery walls elastin is mainly produced during development with a half-life of about 40 years [5]. On the other hand, collagen fibers form a network that exhibits a pronounced hierarchical structure. Collagen molecules are linked to each other by covalent bonds forming fibrils (diameter of about $1.4\,\mathrm{nm}$), which combine to form collagen fibers. The fibers are the main load bearing elements of artery walls and render the material properties anisotropic. They turn over continuously with a half-life on the order of

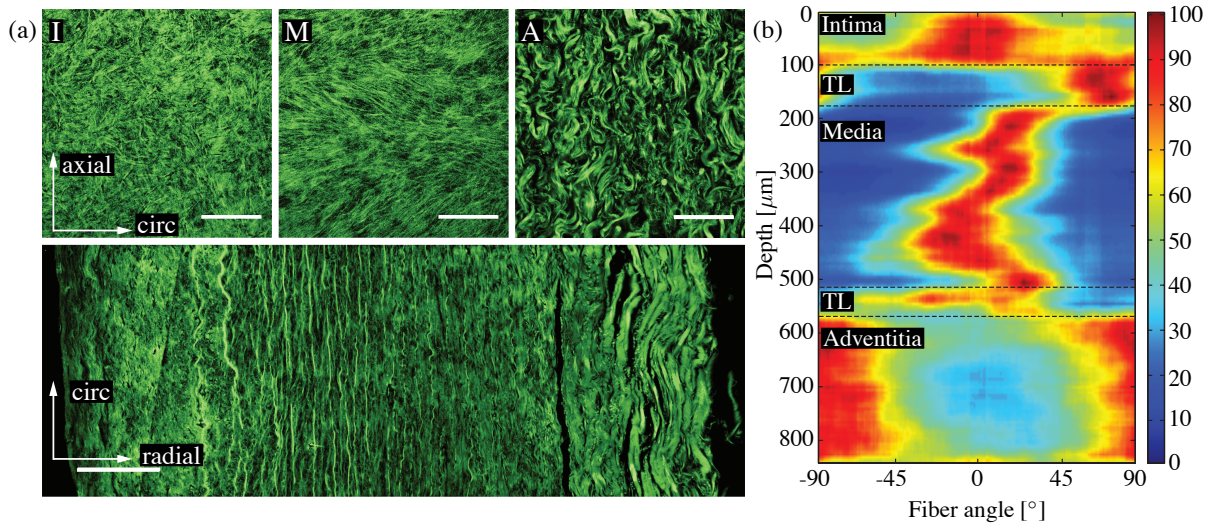

Figure 1: Depiction of the collagen fiber structure through a typical aged healthy human abdominal aorta highlighting the different structures of the intima (I), media (M) and adventitia (A): (a) the top three images represent circumferential/axial sections through the three layers, and the bottom image displays a through-thickness view; (b) intensity plot illustrating the variation of the collagen fiber directions through the wall, where TL refers to transition layers – blue color relates to no fibers and dark red depicts no dispersion. Adapted from [56].

15 to 90 days [39]. Figure 1(a) shows second-harmonic generation (SHG) images of a healthy human aorta. The top three images display circumferential/axial sections of the intima (I), media (M) and adventitia (A), and the bottom image displays a circumferential/radial section. The structure of the intima is tufted, the collagen fibers in the media are oriented more towards the circumferential direction, while in the adventitia the collagen fibers are wavy and oriented more towards the axial direction. Figure 1(b) displays an intensity plot of the collagen fiber directions and dispersion through the thickness of the wall (a fiber angle of 0° identifies the circumferential direction, and 90° refers to the axial direction). The blue color relates to no fibers and dark red depicts no dispersion. Upon stretching the waviness of the collagen fibers is removed so that the collagen fibers can support tension. Collagen fibers which are not wavy support tension as soon as they are stretched.

In terms of the fiber families embedded in the individual layers the extensive study [68] has documented the presence of two fiber families in each aortic layer, with often a third and sometimes a fourth family in the intima. The same was found for the intima and adventitia

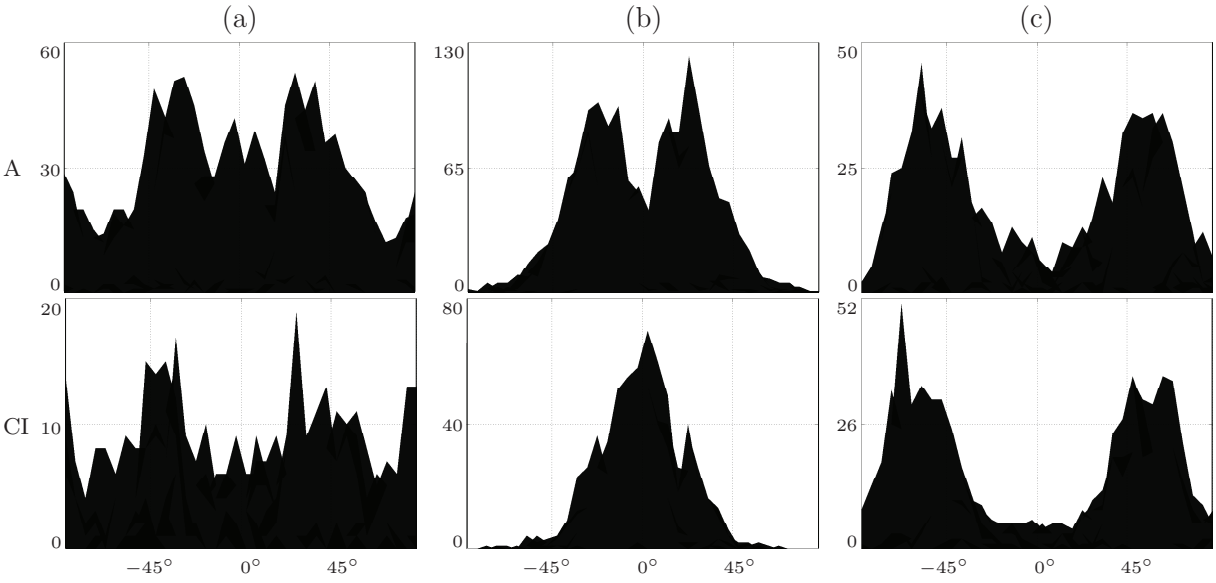

Figure 2: Measured angles in the tangential plane relative to the circumferential direction (identified by $0°$) for abdominal aortas (A), first row, and common iliac arteries (CI), second row; (a) intima, (b) media, and (c) adventitia. Modified from [68].

of common iliac arteries; however, in the media only one family of fibers could be identified with the mean direction oriented circumferentially. The mean fiber directions were always in the tangential plane of the walls, and the out-of-plane dispersion was rather small. Figure 2 provides a layer-specific overview of the measured angles in the tangential plane relative to the circumferential direction (identified by $0°$). These data are obtained from non-atherosclerotic abdominal aortas and common iliac arteries. Polarized light microscopy was used in combination with a universal stage to determine the collagen fiber dispersion for abdominal aortas and common iliac arteries.

The microstructure, in particular in the collagen fabric in diseased tissues, is remarkably different from that of a healthy tissue, as in the case of, e.g., an atherosclerotic tissue; see Fig. 3 modified from [82]. Figure 3(a) shows a histological image of a healthy sample of an iliac artery from an Ossabaw pig, stained for collagen (blue) using Masson's trichrome stain, while Fig. 3(b) shows a corresponding image for an atherosclerotic sample. Note the unstructured collagen arrangement in (b) compared with the more structured arrangement in (a). Another example relates to abdominal aortic aneurysms. It was shown recently that the out-of-plane dispersion in walls of abdominal aortic aneurysms (AAAs) is significantly higher than for tis-

sues obtained from healthy samples [56]. In addition, the characteristic wall structure (intima, media, adventitia) is mainly lost. Remarkably, the waviness of collagen fibers was no longer evident in the abluminal layers of AAAs, and they exhibited rather straight and thick struts of collagen. A comparison of the micro-architecture of ascending thoracic aortas and ascending thoracic aortic aneurysms is discussed in [79].

Figure 4(a) shows two patches taken from each of two adjacent locations of a AAA sample (labeled AAA-4), indicating an intact abluminal layer AL (similar to a healthy adventitia layer). No media was visible as the wavy collagen fibers were infiltrated with plaque and adipocytes. The image LL-1 (LL stands for luminal layer) exhibits bright 'stains' which represent a degenerated collagen structure, while image LL-2, an adjacent region in the same luminal layer, indicates a different structure with calcification and wavy collagen fibers. Figure 4(b) shows another sample (labeled AAA-10), which is obtained from a ruptured AAA. This indicates a significant amount of cystic medial degeneration, infiltrated with adiposytes in the AL. In the LL there is a highly organized collagen structure oriented more towards the circumferential direction. For each of Fig. 4(a) and (b) the intensity plots show the changing collagen fiber orientation through the wall from the LL to the AL. The change in the microstructure with disease clearly has an influence on the mechanical response. Hence, there is a need to consider the structural differences within material models in order for simulations for diseased tissues to better predict the actual *in vivo* stress state.

Mechanical Behavior. The mechanical response of artery walls is governed by both a passive contribution, which is mainly from the elastin and collagen combination, and an active contribution from the SMCs. Key features are that artery walls are anisotropic and behave in a highly nonlinear fashion (soft at low blood pressure with an increasing stiffness at higher pressures) [39]. A typical cylindrical segment of a human artery is subject to a pre-stretch *in vivo* and exhibits no axial deformation under passive cyclic loading, which means that pre-stretches, which change with age and disease, have a significant influence on the mechanical response [69]. This peculiar behavior is a result of the elastin and collagen microstructures and is associated with the anisotropy. Residual stresses, which are best quantified in terms of stretch and curvature [37], are present in unloaded arteries. They arise from development, change with age and disease and also have a significant effect on the *in vivo* stress-strain distribution. The

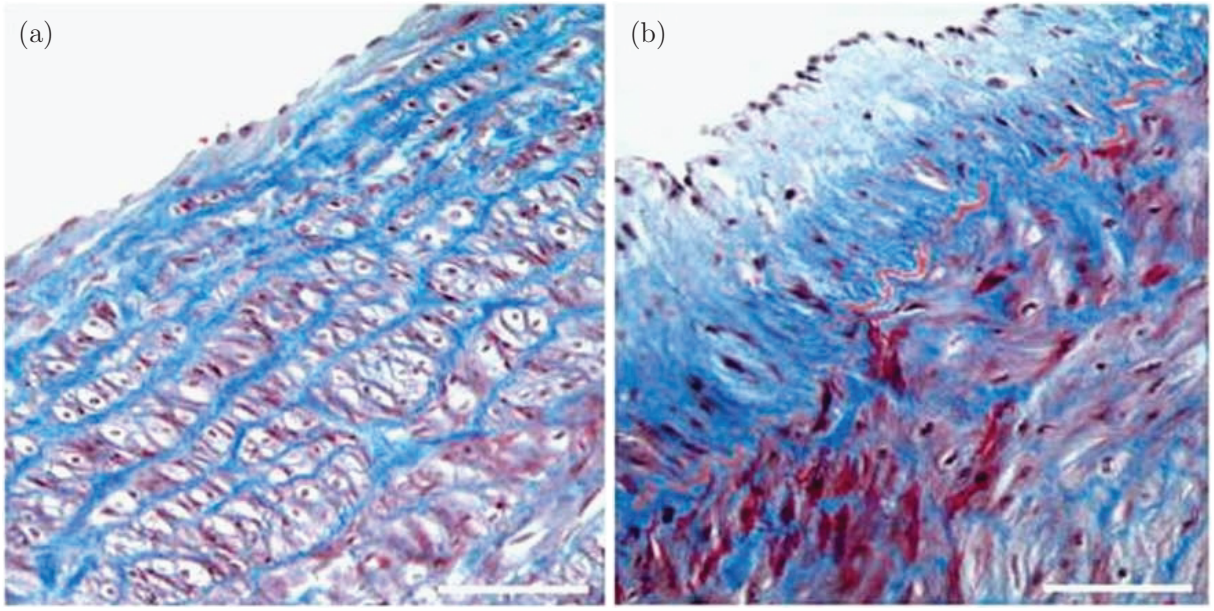

Figure 3: Histological images of iliac arteries from Ossabaw pigs stained for collagen (blue) using Masson's trichrome stain: (a) healthy sample; (b) atherosclerotic sample. Scale bars: 75 μm. Modified from [82].

response of artery walls may also be inelastic; e.g., distal arteries are of the 'muscular type' and have a pronounced viscoelastic behavior [71]; arteries may undergo damage-based softening when they are loaded beyond the physiological range [36], and they may even rupture, as is the case with aortic dissections and aneurysms [41, 87].

The SMCs in the vascular system are responsible for control of short-term changes in lumen diameter and of long-term changes in the extracellular matrix turnover [48], for which fibroblasts play a key role [46]. The gradient of the circumferential stress in the radial direction decreases and the circumferential stress tends to a homeostatic value due to SMC activation, a value which is approximately constant over each layer of the wall [40]. In a homeostatic state SMCs are partially contracted, thus forming the so-called basal tone of the artery. Subsequent contraction and relaxation of SMCs changes the lumen diameter and therefore regulates the resistance to blood flow. Consequently, the mechanical response due to activation is significantly different from the purely passive response, as illustrated in Fig. 5.

The frequency, direction and amount of stretch have been shown to play a major role in the SMC alignment response [50]. A time-dependent reorganization with frequency-dependent

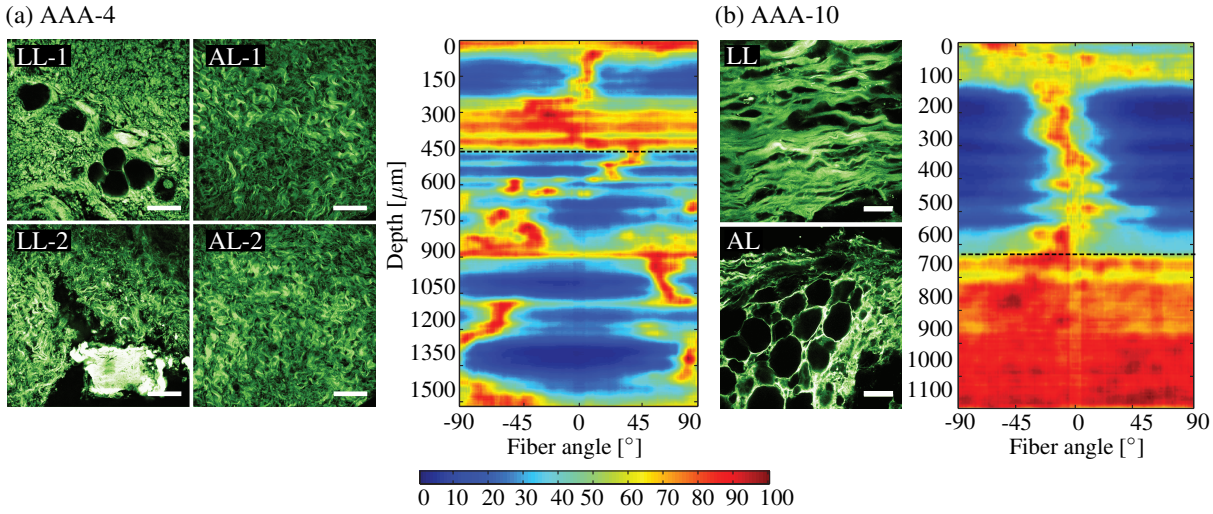

Figure 4: SHG images and intensity plots for two AAA samples (AAA-4, AAA-10): (a) structure of luminal layer, LL-1 and LL-2, and abluminal layer, AL-1 and AL-2, of two patches taken from adjacent locations of sample AAA-4. Image LL-1 exhibits bright 'stains' representing degenerated collagen structures, while image LL-2, indicates a different structure with calcification and wavy collagen fibers. The AL patches are similar to those of a healthy layer. The intensity plot exhibits a highly disturbed structure for the upper $450\,\mu$m and an adventitia-like structure with generally two fiber families in the remaining wall thickness; (b) ruptured sample AAA-10 containing a LL with a highly organized collagen structure and a significant number of adipocytes towards the AL side. The intensity plot shows a collagen structure highly oriented towards the circumferential direction followed by a rather isotropic AL layer. All intensity plots start at the top with the LL. Scale bar is $100\,\mu$m. Modified from [56].

reorientation of SMCs perpendicular to the direction in which the cyclic stretch is applied has been reported in *in vitro* experiments [11, 49]. In vivo experiments performed on basilar arteries of Wistar-Kyoto rats revealed an almost uniform circumferential alignment of SMCs. By contrast, stroke-prone spontaneously hypertensive rats showed a significantly altered distribution and orientation of SMCs [4]. SMCs can produce active tension in the circumferential direction which can be described through a length-tension relationship [13]. They are able to adapt their length-tension behavior relatively quickly when subject to sustained changes in the loading conditions [26, 75, 85]. This adaption process is partly governed by a reorganization of the intracellular filaments. Active stresses exist in the axial direction as well as in the circumfer-

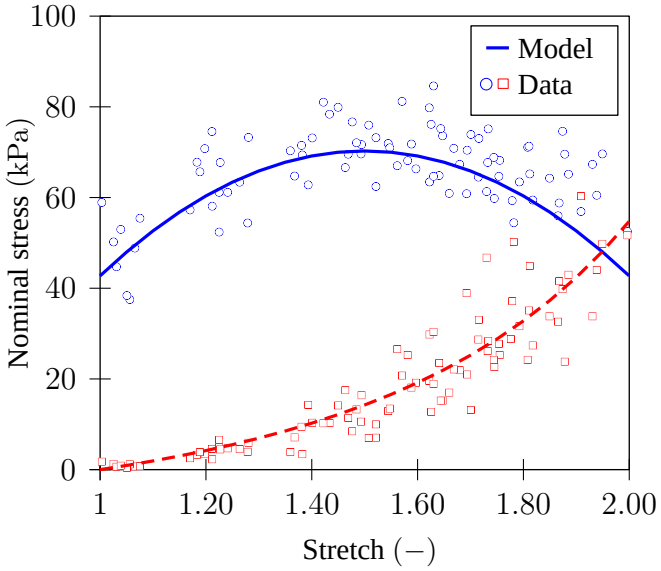

Figure 5: Plots of the uniaxial nominal stress versus stretch of medial strips extracted from pig common carotid arteries. Data are obtained for the active response (blue circles) and passive response (red squares), which are significantly different. The curves represent model fitting according to [53]. Adapted from [53].

ential direction in arteries, which suggests that smooth muscle contraction causes a multiaxial response in vascular walls [2, 10, 54, 76]. Structural investigations suggest that SMCs form two symmetrically and helically arranged families in arteries with an orientation distribution similar to that of collagen fibers [10, 31].

Changes in the (homeostatic) mechanical environment of artery walls such as changes in pressure, flow rate, and axial stretch ratio induce arterial adaptive responses such as growth/atrophy and remodeling [43]. These processes occur hand in hand. Growth/atrophy may be explained as an increase/decrease in mass due to, e.g., an increase/decrease of size or number of cells, while remodeling is a change in mechanical properties and/or structure due to, e.g., a reorganization of existing constituents or a synthesization of new constituents with different organizations. Consequences of growth and remodeling also include hypertrophic SMCs and fragmentation of the internal elastic membrane resulting in an enlarged diameter and wall thickening. In addition, the microstructure may be significantly altered due to disease [56], and hypertension leads to a thickening of the artery wall; basically, thickening is due to hypertrophy of the lamellar units of the media [52].

The typical biomechanical behaviors of fibrous tissues change also with age. For example, SMCs migrate from the media and accumulate in the intima, and this is accompanied by the formation of intimal hyperplasia [81] (the precursor for atherosclerosis), and arteries become stiffer because of the fragmentation and degradation of elastin [61, 23], cross-linking and collagen remodeling (in large arteries the content of collagen increases [44, 78] and the irregularities of arranged fibers in the media increase with age [77]). Finally, aging also affects residual stresses/strains, and in particular the opening angle of a sector formed by a radial cut of an arterial segment increases with age and is larger in vessels with visible atheroma [65, 24, 80, 23].

Material Modeling and Computational Analysis

Microstructural Modeling – Passive Behavior. As shown in the past it is essential to incorporate the microstructure, particularly that generated by the collagen fibers and their dispersed orientation, within a material model [33]. In particular, the character of the dispersion has a very significant influence on the mechanical response of vessel walls. There are basically two approaches that account for the dispersion of collagen fibers. The so-called angular integration approach due to Lanir [45] considers the properties of each fiber to be described by an energy function weighted by an orientation density function and integrated over all orientations. Alternatively, the model developed in [20] is based on the use of a quantity (a so-called structure tensor) that accounts for the distribution of the collagen fibers within a dispersion.

For either model, the energy stored in the fiber structure per unit reference volume, denoted $\Psi_{\rm f}$, can be written compactly is the forms

$$\Psi_{\rm f} = n \int_S \rho(\mathbf{N}) w(\lambda) \mathrm{d}S, \qquad \Psi_{\rm f} = \Psi_{\rm f}(\mathbf{C}, \mathbf{H}), \tag{1}$$

wherein the first expression relates to the angular integration approach, and the second to the structural approach. The notation in (1) is defined as follows. Firstly, the unit vector $\mathbf{N}$ denotes a general direction in the reference configuration, $w(\lambda)$ represents the strain energy of a single collagen fiber in the direction $\mathbf{N}$, λ is the stretch of the fiber in that direction, n is the number of fibers per unit reference volume, $\rho(\mathbf{N})$ is the normalized angular density of fibers, and S denotes the unit sphere over which the integration is performed. In terms of the right Cauchy–Green tensor, which is a measure of the deformation (see, for example, [29]), $\lambda\,(>0)$ is given by $[(\mathbf{C}\mathbf{N})\cdot\mathbf{N}]^{1/2}$. Secondly, in the structural approach, the energy depends on both $\mathbf{C}$ and the

generalized structure tensor $\mathbf{H}$ (independent of the deformation) defined by

$$\mathbf{H} = \frac{1}{4\pi} \int_S \rho(\mathbf{N}) \mathbf{N} \otimes \mathbf{N} \mathrm{d}S, \tag{2}$$

where $\mathbf{N} \otimes \mathbf{N}$ is the tensor product – in components $(\mathbf{N} \otimes \mathbf{N})_{ij} = N_i N_j$. Unfortunately, several of the widely used numerical integration schemes over the unit sphere, as needed for the implementation of $(1)_1$, are inaccurate for large deformation problems, so that a discrete fiber dispersion method in the modeling of artery walls may be superior to a continuous one; see, e.g., the recent study [47] and the references therein. The discrete fiber dispersion model proposed in [47], and illustrated with several examples, also reduces substantially the computational time while maintaining accuracy.

A particular case of the structure tensor (2), describing rotationally symmetric fiber dispersion, was introduced in [20], and has been used for a wide range of different tissues, including arteries. However, more recent data for human non-atherosclerotic thoracic and abdominal aortas and common iliac arteries have shown that the dispersion is not rotationally symmetric [68], and the model in [20] has accordingly been extended in [32] in order to capture the more recent data. In the structural approach [32] one structure tensor is needed for each family of fibers. Each structure tensor is defined by a mean fiber direction, and two dispersion parameters, one describing the out-of-plane fiber dispersion (in the radial direction of an artery), and one in-plane characterizing the fiber dispersion in the tangential plane normal to the radial direction. Thus, in this model there are three structural parameters for each fiber family. The two fiber dispersion parameters can be fitted by using a bivariate von Mises distribution for the orientation density $\rho(\mathbf{N})$, as described in [32].

In [34, 35] we have shown that both model approaches have very similar predictive capabilities, and in these two papers we have also drawn attention to errors propagated in the literature concerning the relative merits of the two model approaches. It is worth noting that either of the basic models in (1) can easily be adapted to account for volume fractions of the constituents and for activation stretches associated with crimped fibers, although this has not always been recognized [8]. In the present review, we focus mainly on the structure tensor approach $(1)_2$, for which the computational analysis is more efficient.

The influence of the values of the two dispersion parameters on a homogeneous biaxial ex-

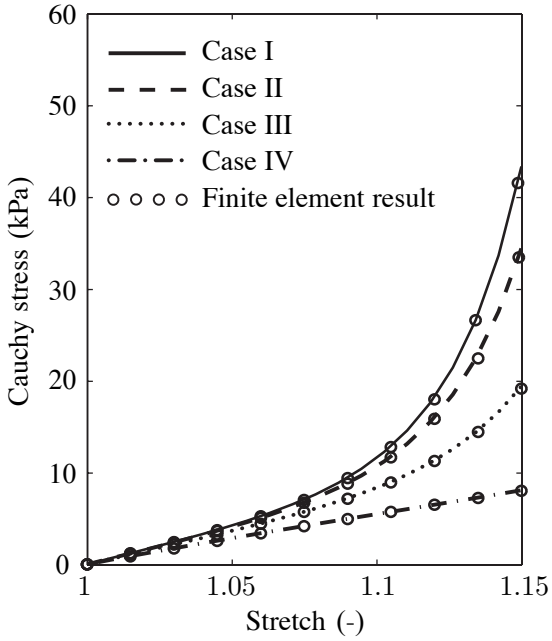

Figure 6: Homogeneous biaxial extension of a cube: plots of the Cauchy stress in the direction of the extension versus stretch in the loading direction. The four different cases of fiber dispersion are described in the text. Modified from [56], with corrected values for the stress.

tension test of a cube is illustrated in Fig. 6, where the Cauchy stress in the direction of the extension is plotted against the stretch in the loading direction. The circles represent finite element results while the curves are obtained from a MATLAB [1] computation, with four different pairs of values of the dispersion parameters (for detailed numbers, see [32]). Case I refers to an analysis which uses values fitted to data obtained from uniaxial tests from the adventitia of a human non-atherosclerotic abdominal aorta, Case II displays the response of the cube with high alignment out-of-plane and isotropy in-plane, Case III refers to a situation with less alignment out-of-plane and isotropy in-plane, and Case IV to an analysis for which the fibers are isotropic both in-plane and out-of-plane. As can be clearly seen, the stress response varies significantly with the fiber structure.

Due to the waviness and slenderness of the fibers it is often assumed that the matrix alone bears the compressive stress [30] and that individual fibers do not support compression. Compared with the non-exclusion of fibers, the mechanical response when compressed fibers are excluded is significantly different, as shown in, e.g., [35].

This model approach can also be used to capture the mechanical response of diseased tissues

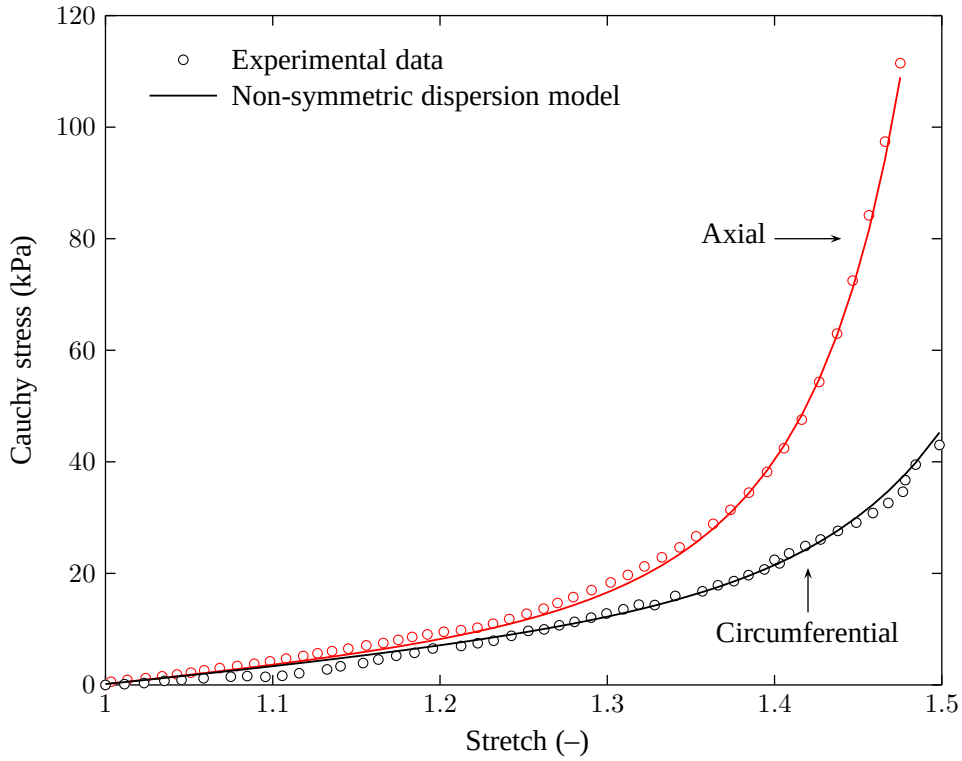

Figure 7: Fitting of the non-symmetric dispersion model [32] to the results of uniaxial extension tests and to images based on picrosirius-polarization in combination with a universal stage. Adapted from [56].

such as that obtained from abdominal aortic aneurysms (AAAs) for which the fiber dispersion is considerably different. In particular, for an AAA the out-of-plane dispersion is significantly increased and, consequently, the set of material and structural parameters changes, as shown in [56].

In order to obtain the structural parameters within $\mathbf{H}$ and the mechanical parameters within $(1)_2$ information is needed about the structure, which can be obtained by imaging analysis, and about the mechanical response obtained from suitable mechanical tests. Ideally, the considered statistical distribution function should be matched with image data to identify the structural parameters, which are then fixed prior to fitting mechanical data. For example, Fig. 7 shows a fit of the non-symmetric dispersion model [32] to the uniaxial stress-stretch data in the circumferential and axial directions. The two samples tested were excised from the adventitia of a human non-atherosclerotic abdominal aorta. The structure of the tissue was identified from 'picrosirius-polarization', in combination with a universal stage [68], while the mechanical properties of the

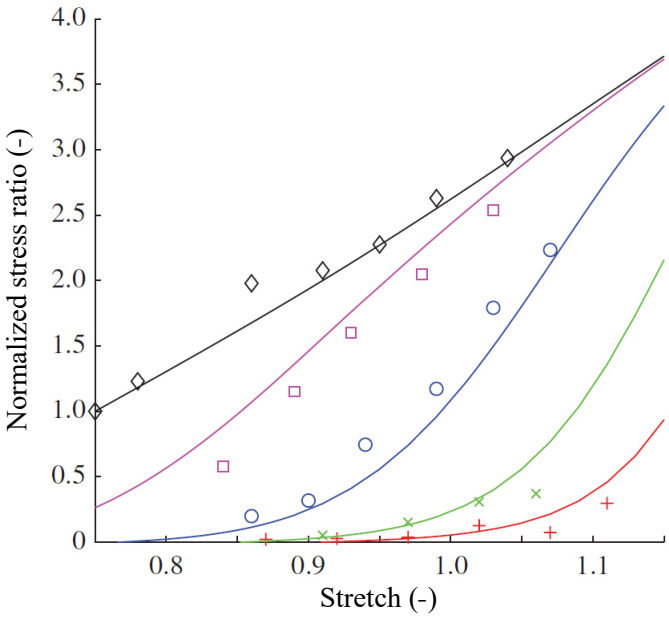

Figure 8: Normalized stress ratio T/T_0 versus stretch for selected calcium ion concentrations $[\mathrm{Ca}]^{2+}$, where T_0 is the minimum value of the stress at the maximally activated state. Data are taken from [42]; red pluses: $[\mathrm{Ca}]^{2+} = 1.9\,\mu$M; green crosses: $[\mathrm{Ca}]^{2+} = 2.7\,\mu$M; blue circles: $[\mathrm{Ca}]^{2+} = 4.3\,\mu$M; pink squares: $[\mathrm{Ca}]^{2+} = 8.9\,\mu$M; black diamonds: $[\mathrm{Ca}]^{2+} > 10\,\mu$M. Related solid curves represent the model results. Adapted from [74].

samples were obtained by performing uniaxial tension tests aligned with the circumferential and axial directions.

Several other microstructure-based models have been developed previously to capture the passive behavior of arteries, and the interested reader is referred to, e.g., [89, 9, 51, 64, 63] (listed in chronological order), to mention just a representative selection.

Cellular Modeling – Active Response. The first model that attempted to describe muscle activation was that in the seminal work of Hill [27]. Papers that describe smooth muscle contractions that are based on Hill's model include, e.g., [21, 25, 86, 90], while the work of Stålhand et al. [74] was the first to use a material law that includes the chemical kinetics of smooth muscles based on the Hai and Murphy model [25] in combination with nonlinear continuum mechanics. Figure 8, taken from [74], illustrates the relationship between the active normalized stress ratio T/T_0 and the stretch for various calcium ion concentrations $[\mathrm{Ca}]^{2+}$, where T_0 denotes the minimum value of the stress at the maximally activated state. For activated muscles, the response is highly nonlinear except for the maximally activated case for which the stress depends linearly

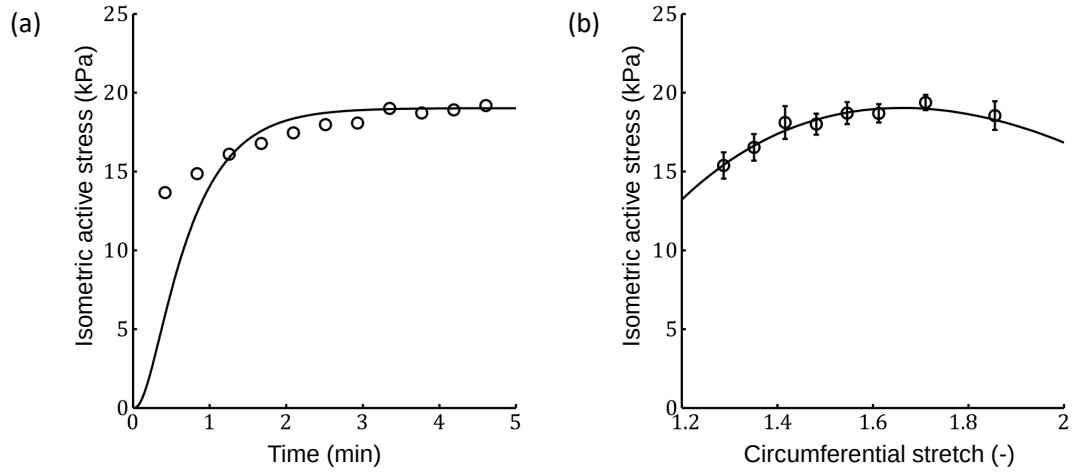

Figure 9: Comparison of experimental data (circles) with model predictions (curves) under isometric contraction: (a) isometric active stress as a function of time (in min) at an optimal circumferential stretch of 1.69; (b) isometric active stress versus circumferential stretch. Adapted from [55].

on the stretch.

In a typical one-dimensional model the total stress T is assumed to have the decoupled form $T = T_{\rm p} + T_{\rm a}$, where $T_{\rm p}$ and $T_{\rm a}$ denote the passive and active contributions, respectively. For 3D models the stress is similarly decoupled, and that is the usual form for models that combine passive and active responses. For a more detailed treatment of active material models up to 2010 see [33]. For more recent developments see, e.g., Murtada et al. [55], in which a new multiscale mathematical model of arterial contractility that accounts for constituents at the molecular, cellular, and tissue levels was proposed. This model is able to capture experimental contraction data in uniaxial and biaxial tests. For example, Fig. 9 illustrates experimental results and predictions of the model. In particular, Fig. 9(a) shows the isometric active stress development at an optimal circumferential stretch of 1.69 over $5\,$min, while Fig. 9(b) depicts the steady-state active stress versus the circumferential stretch.

Conclusions and Open Problems

Considerable progress has been made in the identification of the microstructure and in the modeling of the passive mechanical properties of artery tissues, and to a more limited extent of the active behavior. Much more needs to be learned about changes in the microstructure of artery tissues as they change from the healthy to a diseased state, and the change in the structure

during aging also needs to be better identified. We need to better understand the influence of collagen orientations and diameters, cross-linking between fibers, and mass fractions on the biomechanics of tissues, and how this influence is altered with disease progression. Such information is essential for informing the modeling, simulation and prediction of artery tissue behavior.

For diseases such as AAAs the activation of SMCs is decreased or even completely lost (see, e.g., the review [15], which contains more information on the mechanisms of aneurysm formation and progression). In such a case the fibroblasts in the adventitia are mainly responsible for artery wall remodeling. However, the underlying mechanobiology, which is the study of the biological response of cells to mechanical stimuli [41], requires further investigation to inform constitutive modeling. For diseases such as aortic dissections much remains to be uncovered. In particular, we need to learn more about the mechanical properties and the embedded collagen fiber distribution, including that between aortic layers [58, 72]. We need to better understand what actually triggers an aortic dissection and how to predict the propagation on the basis of a suitable fracture criterion. There is an urgent need to develop more efficient computational tools/algorithms by using clinical images to assist clinicians with diagnosis, treatment, and management of patients.

In addition it is important to determine how the stress distribution in the wall is affected by the density and chemomechanical responses of SMCs. We must better understand how the biology affects the biomechanics of walls in health and disease, and on that basis improved constitutive and computational models are required. For example, the effect of proteoglycans on the biomechanical response of aortic walls is not well studied – only a few studies are available; e.g., in [6] the transmural distribution of proteoglycans has been suggested as a way of regulating residual stresses. In addition, the study [62] documents that the pooling of glycosaminoglycans/proteoglycans can lead to significant stress concentrations and intra-lamellar Donnan-swelling pressures. Another objective is to determine the *in vivo* mechanical properties of tissues, which itself requires knowledge of the *in vivo* microstructure. A recent article reviews the current status in respect of MRI-based *in vivo* identification of biomechanical parameters [73]. In particular, MRI-based biomechanical modeling, and strain imaging may lead to improved risk assessment of carotid artery plaques and may provide input for clinical deci-

sion making. It is also important to better understand the mechanical effects of interventions on tissues which arise from, e.g., the insertion of a stent in an artery, which leads to an adaptive response due to the change in the mechanical environment.

While phenomenological models have played an important role in our initial understanding of the biomechanical response of tissues it is clear that they are no longer sufficient, and it is important that full account is taken of the arterial microstructure in developing constitutive models. However, the fundamental goal is to base constitutive models on a multi-scale approach where mutually supportive simulations and experiments go hand-in-hand in order to advance knowledge and understanding. Hence, the macroscopic mechanical behavior of arteries must be linked to microstructural components, including elastin, collagen fibers, SMCs and the extrafibrillar matrix. Such multi-scale (microstructure-based) models for artery walls, when combined with patient-specific geometries and structures, and imaging data, may be able to better provide (computer-assisted) clinical diagnosis and 3D virtual treatment planning. The imaging data may be obtained from *in vivo* measurements from the cellular and molecular components using advanced multimodality medical imaging. In particular, the continuing developments in imaging science and related image processing algorithms will advance and refine mechanical modeling of artery walls.

In conclusion, we have provided a brief overview of the biomechanical relevance of the microstructure on the passive and active response of artery walls. We hope that this stimulates research towards a better characterization of the biomechanical aspects of arteries, which will then allow for a better understanding of cardiovascular biomechanics and pathophysiology.

References

[1] MATLAB, 2016. R2016a, The MathWorks Inc., Natick, MA, USA, 2016.

[2] A. Agianniotis, A. Rachev, and N. Stergiopulos. Active axial stress in mouse aorta. *J. Biomech.*, 45:1924–1927, 2012.

[3] A. C. Akyildiz, C.-K. Chai, C. W. J. Oomens, A. van der Lugt, F. P. T. Baaijens, G. J. Strijkers, and F. J. H. Gijsen. 3D fiber orientation in atherosclerotic carotid plaques. *J.*

Struct. Biol., 200:28–35, 2017.

[4] S. M. Arribas, J. F. Gordon, C. J. Daly, A. F. Dominiczak, and J. C. McGrath. Confocal microscopic characterization of a lesion in a cerebral vessel of the stroke-prone spontaneously hypertensive rat. *Stroke*, 27:1118–1123, 1996.

[5] S. M. Arribas, A. Hinek, and M. C. Gonzalez. Elastic fibres and vascular structure in hypertension. *Pharmacol. Ther.*, 111:771–791, 2006.

[6] E. U. Azeloglu, M. B. Albro, V. A. Thimmappa, G. A. Ateshian, and K. D. Costa. Heterogeneous transmural proteoglycan distribution provides a mechanism for regulating residual stresses in the aorta. *Am. J. Physiol. Heart Circ. Physiol.*, 294:H1197–H1205, 2008.

[7] P. B. Canham, H. M. Finlay, J. G. Dixon, D. R. Boughner, and A. Chen. Measurements from light and polarised light microscopy of human coronary arteries fixed at distending pressure. *Cardiovasc. Res.*, 23:973–982, 1989.

[8] H. Chen and G. S. Kassab. Microstructure-based biomechanics of coronary arteries in health and disease. *J. Biomech.*, 49:2548–2559, 2016.

[9] H. Chen, Y. Liu, X. Zhao, Y. Lanir, and G. S. Kassab. A micromechanics finite-strain constitutive model of fibrous tissue. *J. Mech. Phys. Solids*, 59:1823–1837, 2011.

[10] H. Chen, T. Luo, X. Zhao, X. Lu, Y. Huo, and G. S. Kassab. Microstructural constitutive model of active coronary media. *Biomaterials*, 34:7575–7583, 2013.

[11] Q. Chen, W. Li, Z. Quan, and B. E. Sumpio. Modulation of vascular smooth muscle cell alignment by cyclic strain is dependent on reactive oxygen species and P38 mitogen-activated protein kinase. *J. Vasc. Surg.*, 37:660–668, 2003.

[12] J. M. Clark and S. Glagov. Transmural organization of the arterial media: The lamellar unit revisited. *Arteriosclerosis*, 5:19–34, 1985.

[13] R. H. Cox. Regional variation of series elasticity in canine arterial smooth muscles. *Am. J. Physiol.*, 234:H542–H551, 1978.

[14] C. J. Cyron and J. D. Humphrey. Preferred fiber orientations in healthy arteries and veins understood from netting analysis. *Math. Mech. Solids*, 20:680–696, 2015.

[15] F. M. Davis, D. L. Rateri, and A. Daugherty. Mechanisms of aortic aneurysm formation: translating preclinical studies into clinical therapies. *Heart*, 100:1498–1505, 2014.

[16] H. M. Finlay, L. McCullough, and P. B. Canham. Three-dimensional collagen organization of human brain arteries at different transmural pressures. *J. Vasc. Res.*, 32:301–312, 1995.

[17] H. M. Finlay, P. Whittaker, and P. B. Canham. Collagen organization in the branching region of human brain arteries. *Stroke*, 29:1595–1601, 1998.

[18] T. Fujiwara and Y. Uehara. The cytoarchitecture of the medial layer in rat thoracic aorta: a scanning electron-microscopic study. *Connect. Tissue Res.*, 270:165–172, 1992.

[19] T. C. Gasser, S. Gallinetti, X. Xing, C. Forsell, J. Swedenborg, and J. Roy. Spatial orientation of collagen fibers in the abdominal aortic aneurysm's wall and its relation to wall mechanics. *Acta Biomater.*, 8:3091–3103, 2012.

[20] T. C. Gasser, R. W. Ogden, and G. A. Holzapfel. Hyperelastic modelling of arterial layers with distributed collagen fibre orientations. *J. R. Soc. Interface*, 3:15–35, 2006.

[21] S. Gestrelius and P. Borgström. A dynamic model of smooth muscle contraction. *Biophys. J.*, 50:157–169, 1986.

[22] S. Ghazanfari, A. Driessen-Mol, G. J. Strijkers, F. M. W. Kanters, F. P. T. Baaijens, and C. V. C. Bouten. A comparative analysis of the collagen architecture in the carotid artery: Second harmonic generation versus diffusion tensor imaging. *Biochem. Biophys. Res. Commun.*, 426:54–58, 2012.

[23] S. E. Greenwald. Ageing of the conduit arteries. *J. Pathol.*, 211:157–172, 2007.

[24] S. E. Greenwald, J. E. Moore, Jr., A. Rachev, T. P. C. Kane, and J.-J. Meister. Experimental investigation of the distribution of residual strains in the artery wall. *J. Biomech. Eng.*, 119:438–444, 1997.

[25] C.-M. Hai and R. A. Murphy. Cross-bridge phosphorylation and regulation of latch state in smooth muscle. *J. Appl. Physiol.*, 254:C99–106, 1988.

[26] A. M. Herrera, B. E. McParland, A. Bienkowska, R. Tait, P. D. Paré, and C. Y. Seow. Sarcomeres of smooth muscle: functional characteristics and ultrastructural evidence. *J. Cell Sci.*, 118:2381–2392, 2005.

[27] A. V. Hill. The heat of shortening and the dynamic constants of muscle. *Proc. R. Soc. Lond. B*, 126:136–195, 1938.

[28] M. R. Hill, X. Duan, G. A. Gibson, S. Watkins, and A. M. Robertson. A theoretical and non-destructive experimental approach for direct inclusion of measured collagen orientation and recruitment into mechanical models of the artery wall. *J. Biomech.*, 45:762–771, 2012.

[29] G. A. Holzapfel. *Nonlinear Solid Mechanics. A Continuum Approach for Engineering*. John Wiley & Sons, Chichester, 2000.

[30] G. A. Holzapfel, T. C. Gasser, and R. W. Ogden. A new constitutive framework for arterial wall mechanics and a comparative study of material models. *J. Elasticity*, 61:1–48, 2000.

[31] G. A. Holzapfel, T. C. Gasser, and M. Stadler. A structural model for the viscoelastic behavior of arterial walls: Continuum formulation and finite element analysis. *Eur. J. Mech. A/Solids*, 21:441–463, 2002.

[32] G. A. Holzapfel, J. A. Niestrawska, R. W. Ogden, A. J. Reinisch, and A. J. Schriefl. Modelling non-symmetric collagen fibre dispersion in arterial walls. *J. R. Soc. Interface*, 12:2015–0188, 2015.

[33] G. A. Holzapfel and R. W. Ogden. Constitutive modelling of arteries. *Proc. R. Soc. Lond. A*, 466:1551–1597, 2010.

[34] G. A. Holzapfel and R. W. Ogden. Comparison of two model frameworks for fiber dispersion in the elasticity of soft biological tissues. *Eur. J. Mech. A/Solids*, 66:193–200, 2017.

[35] G. A. Holzapfel and R. W. Ogden. On fiber dispersion models: exclusion of compressed fibers and spurious model comparisons. *J. Elasticity*, 129:49–68, 2017.

[36] G. A. Holzapfel, C. A. J. Schulze-Bauer, and M. Stadler. Mechanics of angioplasty: Wall, balloon and stent. In J. Casey and G. Bao, editors, *Mechanics in Biology*, New York, 2000. The American Society of Mechanical Engineers (ASME). AMD-Vol. 242/BED-Vol. 46, pp. 141–156.

[37] G. A. Holzapfel, G. Sommer, M. Auer, P. Regitnig, and R. W. Ogden. Layer-specific 3D residual deformations of human aortas with non-atherosclerotic intimal thickening. *Ann. Biomed. Eng.*, 35:530–545, 2007.

[38] G. A. Holzapfel, G. Sommer, C. T. Gasser, and P. Regitnig. Determination of layer-specific mechanical properties of human coronary arteries with non-atherosclerotic intimal thickening, and related constitutive modeling. *Am. J. Physiol. Heart Circ. Physiol.*, 289:H2048–2058, 2005.

[39] J. D. Humphrey. *Cardiovascular Solid Mechanics. Cells, Tissues, and Organs*. Springer-Verlag, New York, 2002.

[40] J. D. Humphrey. Native properties of cardiovascular tissues: Guidlines of functional tissue engineering. In F. Guilak, D. L. Butler, St. A. Goldstein, and D. J. Mooney, editors, *Functional Tissue Engineering*, pages 35–45, New York, 2003. Springer-Verlag.

[41] J. D. Humphrey and G. A. Holzapfel. Mechanics, mechanobiology, and modeling of human abdominal aorta and aneurysms. *J. Biomech.*, 45:805–814, 2012.

[42] P. J. Hunter, A. D. McCulloch, and H. E. D. J. ter Keurs. Modelling the mechanical properties of cardiac muscle. *Prog. Biophys. Mol. Biol.*, 69:289–331, 1998.

[43] Z. S. Jackson, A. I. Gotlieb, and B. L. Langille. Wall tissue remodeling regulates longitudinal tension in arteries. *Circ. Res.*, 90:918–925, 2002.

[44] E. G. Lakatta. Cardiovascular aging in health. *Clin. Geriatr. Med.*, 16:419–444, 2000.

[45] Y. Lanir. Constitutive equations for fibrous connective tissues. *J. Biomech.*, 16:1–12, 1983.

[46] G. J. Laurent, R. C. Chambers, M. R. Hill, and R. J. McAnulty. Regulation of matrix turnover: fibroblasts, forces, factors and fibrosis. *Biochem. Soc. Trans.*, 35:647–651, 2007.

[47] K. Li, R. W. Ogden, and G. A. Holzapfel. A discrete fibre dispersion method for excluding fibres under compression in the modelling of fibrous tissues. *J. R. Soc. Interface*, 15:20170766, 2018.

[48] Q. Li, Y. Muragaki, I. Hatamura, H. Ueno, and A. Ooshima. Stretch-induced collagen synthesis in cultured smooth muscle cells from rabbit aortic media and a possible involvement of angiotensin II and transforming growth factor-β. *J. Vasc. Res.*, 35:93–103, 1998.

[49] B. Liu, M. J. Qu, K. R. Qin, H. Li, Z. K. Li, B. R. Shen, and Z. L. Jiang. Role of cyclic strain frequency in regulating the alignment of vascular smooth muscle cells in vitro. *Biophys. J.*, 94:1497–1507, 2008.

[50] L. E. Mantella, A. Quan, and S. Verma. Variability in vascular smooth muscle cell stretch-induced responses in 2D culture. *Vasc. Cell*, 7:7, 2015.

[51] G. Martufi and T. C. Gasser. A constitutive model for vascular tissue that integrates fibril, fiber and continuum levels with application to the isotropic and passive properties of the infrarenal aorta. *J. Biomech.*, 44:2545–2550, 2011.

[52] T. Matsumoto and K. Hayashi. Stress and strain distribution in hypertensive and normotensive rat aorta considering residual strain. *J. Biomech.*, 118:62–73, 1996.

[53] S. C. Murtada, A. Arner, and G. A. Holzapfel. Experiments and mechanochemical modeling of smooth muscle contraction: significance of filament overlap. *J. Theor. Biol.*, 297:176–186, 2012.

[54] S.-I. Murtada, J. Ferruzzi, H. Yanagisawa, and J. D. Humphrey. Reduced biaxial contractility in the descending thoracic aorta of fibulin-5 deficient mice. *J. Biomech. Eng.*, 138:051008, 2016.

[55] S.-I. Murtada, J. D. Humphrey, and G. A. Holzapfel. Multiscale and multiaxial mechanics of vascular smooth muscle. *Biophys. J.*, 113:714–727, 2017.

[56] J. A. Niestrawska, Ch. Viertler, P. Regitnig, T. U. Cohnert, G. Sommer, and G. A. Holzapfel. Microstructure and mechanics of healthy and aneurysmatic abdominal aortas: experimental analysis and modeling. *J. R. Soc. Interface*, 13:2016–0620, 2016.

[57] M. K. O'Connell, S. Murthy, S. Phan, C. Xu, J. Buchanan, R. Spilker, R. L. Dalman, C. K. Zarins, W. Denk, and C. A. Taylor. The three–dimensional micro– and nanostructure of the aortic medial lamellar unit measured using 3D confocal and electron microscopy imaging. *Matrix Biol.*, 27:171–181, 2008.

[58] S. Pal, A. Tsamis, S. Pasta, A. D'Amore, T. G. Gleason, D. A. Vorp, and S. Maiti. A mechanistic model on the role of radially-running collagen fibers on dissection properties of human ascending thoracic aorta. *J. Biomech.*, 47:981–988, 2014.

[59] J. A. G. Rhodin. Architecture of the vessel wall. In R. M. Berne, editor, *Handbook of Physiology, Section 2, Volume 2*. Am Physiol Soc, Bethesda, 1979.

[60] M. R. Roach and A. C. Burton. The reason for the shape of the distensibility curves of arteries. *Canad. J. Biochem. Physiol.*, 35:681–690, 1957.

[61] L. Robert. Aging of the vascular wall and atherogenesis: role of the elastin-laminin receptor. *Atherosclerosis*, 123:169–179, 1996.

[62] S. Roccabianca, G. A. Ateshian, and J. D. Humphrey. Biomechanical roles of medial pooling of glycosaminoglycans in thoracic aortic dissection. *Biomech. Model. Mechanobiol.*, 13:13–25, 2014.

[63] P. Sáez, A. García, E. Peña, T. C. Gasser, and M. A. Martínez. Microstructural quantification of collagen fiber orientations and its integration in constitutive modeling of the porcine carotid artery. *Acta Biomater.*, 33:183–193, 2016.

[64] P. Sáez, E. Peña, and M. A. Martínez. A structural approach including the behavior of collagen cross-links to model patient-specific human carotid arteries. *Ann. Biomed. Eng.*, 42:1158–1169, 2014.

[65] A. Saini, C. Berry, and S. Greenwald. Effect of age and sex on residual stress in the aorta. *J. Vasc. Res.*, 32:398–405, 1995.

[66] A. J. Schriefl, A. J. Reinisch, S. Sankaran, D. M. Pierce, and G. A. Holzapfel. Quantitative assessment of collagen fiber orientations from 2D images of soft biological tissues. *J. R. Soc. Interface*, 9:3081–3093, 2012.

[67] A. J. Schriefl, H. Wolinski, P. Regitnig, S. D. Kohlwein, and G. A. Holzapfel. An automated approach for three-dimensional quantification of fibrillar structures in optically cleared soft biological tissues. *J. R. Soc. Interface*, 10:2012–0760, 2013.

[68] A. J. Schriefl, G. Zeindlinger, D. M. Pierce, P. Regitnig, and G. A. Holzapfel. Determination of the layer-specific distributed collagen fiber orientations in human thoracic and abdominal aortas and common iliac arteries. *J. R. Soc. Interface*, 9:1275–1286, 2012.

[69] C. A. J. Schulze-Bauer and G. A. Holzapfel. Determination of constitutive equations for human arteries from clinical data. *J. Biomech.*, 36:165–169, 2003.

[70] C. A. J. Schulze-Bauer, P. Regitnig, and G. A. Holzapfel. Mechanics of the human femoral adventitia including high-pressure response. *Am. J. Physiol. Heart Circ. Physiol.*, 282:H2427–H2440, 2002.

[71] F. H. Silver, I. Horvath, and D. J. Foran. Viscoelasticity of the vessel wall: the role of collagen and elastic fibers. *Crit. Rev. Biomed. Eng.*, 29:279–301, 2001.

[72] G. Sommer, S. Sherifova, P. J. Oberwalder, O. E. Dapunt, P. A. Ursomanno, A. DeAnda, B. E. Griffith, and G. A. Holzapfel. Mechanical strength of aneurysmatic and dissected human thoracic aortas at different shear loading modes. *J. Biomech.*, 49:2374–2382, 2016.

[73] L. Speelman, Z. Teng, A. J. Nederveen, A. van der Lugt, and J. H. Gillard. MRI-based biomechanical parameters for carotid artery plaque vulnerability assessment. *Thrombosis and Haemostasis*, 115:493–500, 2016.

[74] J. Stålhand, A. Klarbring, and G. A. Holzapfel. Smooth muscle contraction: mechanochemical formulation for homogeneous finite strains. *Prog. Biophys. Mol. Biol.*, 96:465–481, 2008.

[75] H. Syyong, C. Cheung, D. Solomon, C. Y. Seow, and K. H. Kuo. Adaptive response of pulmonary arterial smooth muscle to length change. *J. Appl. Physiol.*, 104:1014–1020, 2008.

[76] K. Takamizawa, K. Hayashi, and T. Matsuda. Isometric biaxial tension of smooth muscle in isolated cylindrical segments of rabbit arteries. *Am. J. Physiol.*, 263:H30–H34, 1992.

[77] T. Toda, N. Tsuda, I. Nishimori, D. E. Leszczynski, and F. A. Kummerow. Morphometrical analysis of the aging process in human arteries and aorta. *Acta Anat. (Basel)*, 106:35–44, 1980.

[78] A. Tsamis, J. T. Krawiec, and D. A. Vorp. Elastin and collagen fibre microstructure of the human aorta in ageing and disease: a review. *J. R. Soc. Interface*, 10:20121004, 2013.

[79] A. Tsamis, J. A. Phillippi, R. G. Koch, S. Pasta, A. D'Amore, S. C. Watkins, W. R. Wagner, T. G. Gleason, and D. A. Vorp. Fiber micro-architecture in the longitudinal-radial and circumferential-radial planes of ascending thoracic aortic aneurysm media. *J. Biomech.*, 46:2787–2794, 2013.

[80] J. Valenta, K. Vitek, R. Cihák, S. Konvickova, M. Sochor, and L. Horny. Age related constitutive laws and stress distribution in human main coronary arteries with reference to residual strain. *Biomed. Mater. Eng.*, 12:121–134, 2002.

[81] C. Velican and D. Velican. Study of coronary intimal thickening. *Atherosclerosis*, 56:331–344, 1985.

[82] S. R. Watson and S. M. Lessner. (second) harmonic disharmony: nonlinear microscopy shines new light on the pathology of atherosclerosis. *Microsc. Microanal.*, 22:589–598, 2016.

[83] P. N. Watton, Y. Ventikos, and G. A. Holzapfel. Modelling the mechanical response of elastin for arterial tissue. *J. Biomech.*, 42:1320–1325, 2009.

[84] H. Weisbecker, C. Viertler, D. M. Pierce, and G. A. Holzapfel. The role of elastin and collagen in the softening behavior of the human thoracic aortic media. *J. Biomech.*, 46:1859–1865, 2013.

[85] R. Yamin and K. G. Morgan. Deciphering actin cytoskeletal function in the contractile vascular smooth muscle cell. *J. Physiol.*, 590:4145–4154, 2012.

[86] J. Yang, J. W. Clark Jr., R. M. Bryan, and C. Robertson. The myogenic response in isolated rat cerebrovascular arteries: smooth muscle cell model. *Med. Eng. Phys.*, 25:691–709, 2003.

[87] P. Youssefi, R. Sharma, C. A. Figueroa, and M. Jahangiri. Functional assessment of thoracic aortic aneurysms – the future of risk prediction? *Br. Med. Bull.*, 121:61–71, 2017.

[88] Y. Zou and Y. Zhang. An experimental and theoretical study on the anisotropy of elastin network. *Ann. Biomed. Eng.*, 37:1572–1583, 2009.

[89] M. A. Zulliger, P. Fridez, K. Hayashi, and N. Stergiopulos. A strain energy function for arteries accounting for wall composition and structure. *J. Biomech.*, 37:989–1000, 2004.

[90] M. A. Zulliger, A. Rachev, and N. Stergiopulos. A constitutive formulation of arterial mechanics including vascular smooth muscle tone. *Am. J. Physiol. Heart Circ. Physiol.*, 287:H1335–1343, 2004.